remote sensing

MDPI

Article

Remote Sensing of Water Use Efficiency and Terrestrial Drought Recovery across the Contiguous United States

Behzad Ahmadi [1,*], Ali Ahmadalipour [2], Glenn Tootle [2] and Hamid Moradkhani [2,*]

[1] Department of Civil and Environmental Engineering, Portland State University, Portland, OR 97201, USA
[2] Center for Complex Hydrosystems Research, Department of Civil, Construction and Environmental Engineering, University of Alabama, Tuscaloosa, AL 35487, USA; aahmada@eng.ua.edu (A.A.); gatootle@eng.ua.edu (G.T.)
* Correspondence: bahmadi@pdx.edu (B.A.); hmoradkhani@ua.edu (H.M.)

Received: 29 January 2019; Accepted: 18 March 2019; Published: 26 March 2019

Abstract: Ecosystem water-use efficiency (WUE) is defined as the ratio of carbon gain (i.e., gross primary productivity; GPP) to water consumption (i.e., evapotranspiration; ET). WUE is markedly influential on carbon and water cycles, both of which are fundamental for ecosystem state, climate and the environment. Drought can affect WUE, subsequently disturbing the composition and functionality of terrestrial ecosystems. In this study, the impacts of drought on WUE and its components (i.e., GPP and ET) are assessed across the Contiguous US (CONUS) at fine spatial and temporal resolutions. Soil moisture simulations from land surface modeling are utilized to detect and characterize agricultural drought episodes and remotely sensed GPP and ET are retrieved from the moderate resolution imaging spectroradiometer (MODIS). GPP, as the biome vitality indicator against drought stress, is employed to investigate drought recovery and the ecosystems' required time to revert to pre-drought condition. Results show that drought recovery duration indicates a positive correlation with drought severity and duration, meaning that a protracted drought recovery is more likely to happen following severe droughts with prolonged duration. WUE is found to almost always increase in response to severe (or worse) drought episodes. Additionally, ET anomalies are negatively correlated with drought severity and ET is expected to decrease during severe (or worse) drought episodes. Lastly, the changes of WUE are decomposed in relation to its components and the cross-relation among the variables is revealed and a consistent changing pattern is detected.

Keywords: drought; Water Use Efficiency; gross primary productivity; evapotranspiration; drought recovery; CONUS

1. Introduction

Drought, as a prolonged period of moisture deficiency in land surface, affects terrestrial ecosystems from structural and functional perspectives (i.e., constraining vegetation growth, causing plant mortality and triggering wildfire), which leads to profound imbalances in the terrestrial carbon cycle [1–4]. In addition, climate change, which is a consequence of increased greenhouse gas emission and global warming [5–7], will exacerbate drought frequency and severity in the 21st century [8–11].

Drought is generally categorized to four types: Meteorological Drought, Agricultural Drought, Hydrological Drought and Socioeconomic Droughts. An agricultural drought indicates a deficit in soil moisture and thus it can happen in any land cover. An agricultural drought onset is typically perceived when the soil moisture level drops below a threshold causing crop water stress (affecting crop yield). Consequently, soil moisture is regarded as an indicator of agricultural drought [12–14]. Spatially varying precipitation, land cover, soil and topography cause heterogeneity, which makes

soil moisture estimation from field measurement complicated [15,16]. Therefore, land surface models and/or remotely sensed observations are often adopted to estimate soil moisture. There are many studies utilizing land surface models to estimate soil moisture and analyze historical agricultural drought episodes [17–19]. Additionally, remote sensing advances have provided major soil moisture data availability at global scale [20], which facilitates obtaining precise and frequent soil moisture maps globally [21,22]. There are several studies, which compared agricultural drought analysis obtained from in situ and remotely sensed soil moisture data [23–25]. Some studies combined land surface models simulations with remotely sensed data to minimize the uncertainty of soil moisture estimation [26,27]. Recent studies by Yan et al. [28,29] have assimilated remotely sensed soil moisture observations to land surface models in order to improve the accuracy of soil moisture simulations and drought monitoring.

Ecosystem Water Use Efficiency (WUE) is defined as the ratio of carbon gain (i.e., Gross Primary Productivity; GPP) to water consumption (i.e., Evapotranspiration; ET), which links biological and water cycles over the land surface (WUE = GPP/ET) [30,31]. GPP as a key component of the terrestrial carbon cycle, represents the sum of gross carbon (CO_2) uptake by plant photosynthesis [32,33]. Theoretically, the ecological transpiration is the true water consumption by plant photosynthesis. However, due to the infeasibility of distinguishing soil and canopy evaporation and plant transpiration from evapotranspiration (ET) [34], either precipitation [35] or ET [36] are used as indicators of water loss (i.e., consumed by the ecosystem). Among various definitions of WUE, the GPP/ET is the most common indicator and it is employed in this study too [1,3,37].

WUE is a key variable to understand the response of ecosystem productivity to any physical changes (e.g., water availability, climate change, etc.). Droughts can be associated with heatwaves and decreased water availability [38,39], which may result in either increase or reduction of evapotranspiration, respectively, leading to significant disruptions in the global water balance and may cause permanent changes to the ecosystems [40,41].

The WUE alteration and its effects on the ecosystem resilience to drought disturbances have been investigated in recent studies [1,3,35,42]. Regional assessments have concluded that ecosystem biomes are able to enhance their WUE in order to cope with water stress [36]. However, such a conclusion has been challenged by several large-scale investigations implying that the response of WUE to drought depends on the vegetation condition and climate [1,3,30]. Therefore, more investigation is still needed to understand WUE-drought relations and reveal the spatiotemporal patterns and influential factors.

Drought recovery duration is often assumed to be rapid. In some studies, drought recovery is assessed focusing on the required precipitation to recover from a drought episode [43,44], whereas few studies elaborated on drought recovery considering restoring function of plants [45,46]. From a hydrological perspective, a region is assumed to recover from drought when the hydrologic variable of interest (e.g., streamflow) reverts to its pre-drought level [47]. Schwalm et al. [48] stated that recovery time is the duration that "an ecosystem requires to revert to its pre-drought condition." Understanding drought recovery duration is critical for ecosystem, since if a region experiences a new drought episode before full recovery from an antecedent drought event, the ecosystem may experience substantial permanent ecological impacts [49,50].

In this study, the relationships between agricultural droughts and ecosystem WUE is examined using land surface soil moisture simulations as well as remotely sensed GPP and ET products. The root-zone soil moisture percentile is utilized to characterize drought episodes across the contiguous United States. We investigate the response of WUE and its components to drought across different regions. Additionally, terrestrial drought recovery duration is also assessed for various drought events with diverse intensities.

2. Materials and Method

2.1. Remotely Sensed Data

The 8-day GPP [51,52] and ET [53,54] data with 1-km spatial resolution are acquired from the MODIS instrument onboard Terra satellite during 2000 to 2014, from the Numerical Terradynamic Simulation Group (http://www.ntsg.umt.edu). The MODIS GPP product (MOD17A2) was developed based on a light-use efficiency model [55]. GPP is the largest contributor of carbon flux and the largest carbon uptake by terrestrial ecosystems.

Many studies have confirmed the accuracy and validity of MODIS GPP [56–61] and it is compared with station observations in many regions and biomes [52,56,62]. The MODIS GPP product has been widely used in studies with various spatial scales and domains (regional to global) in different ecosystems [63,64].

The Penman-Monteith model was adopted to estimate the global MODIS ET product (MOD16A2), which uses meteorological reanalysis data and vegetation property dynamics (e.g., land cover, leaf area index and albedo). The forcing data for the model are retrieved from the MODIS data [54,65]. The validation of MODIS ET product using station flux tower data showed reasonable accuracy over the Contiguous United States (CONUS) [65,66].

In addition to GPP and ET, the biome types over the CONUS are determined according the MODIS global land cover product (MCD12Q1) acquired from the global land cover facility of the University of Maryland (http://glcf.umd.edu/data/lc/). In this study, the biomes are classified into 10 types as follows: Evergreen Needleleaf Forest (ENF), Evergreen Broadleaf Forest (EBF), Deciduous Needleleaf Forest (DNF), Deciduous Broadleaf Forest (DBF), Mixed forest, Shrublands, Savannas, Grasslands, Croplands/natural vegetation and Wetlands. The original spatial resolution of biomes are 500 m, which are aggregated to 1-km in order to be consistent with the GPP and ET datasets.

2.2. Simulated Data

In this study, soil moisture simulations from the Phase 2 of the North American Land Data Assimilation System (NLDAS-2) are utilized over the CONUS from 1983 to 2014 with an 8-day temporal resolution and spatial resolution of 1/8° (about 12km). The data is available over the north America from 1979 to present [67]. Soil moisture states are simulated using the semi-distributed grid-based model Variable Infiltration Capacity (VIC) [68,69] which is a macroscale hydrologic model that ingests meteorological forcing data and solves for full water and energy balances. A Soil-Vegetation-Atmosphere Transfer (SVAT) scheme controls the moisture and energy fluxes within VIC and in comparison with most SVATs, it reproduces the runoff characteristics more accurately [70]. In the NLDAS-2 dataset, VIC model was run at a spatial resolution of 1/8° with full energy balance mode at hourly time step. It also represents sub-grid variability of vegetation and runoff generation [71]. The version of the VIC model used for the NLDAS-2 is VIC-4.0.3. The vadose (unsaturated) zone in each grid cell is partitioned into three layers with a depth of 10 cm for the top layer and varying depths for other layers. Table 1 represents a summary of all the data products used in this study and their characteristics.

Table 1. Summary of the data used in this study and their characteristics.

Data	Original Spatial Resolution	Temporal Resolution	Unit	Type
Gross Primary Productivity (GPP) (MOD17A2)	1 km	8 days	kgC/m^2	Remotely sensed by MODIS
Evapotranspiration (ET) (MOD16A2)	1 km	8 days	mm	Remotely sensed by MODIS
Land Cover (MCD12Q1)	500 m	monthly	——	Remotely sensed by MODIS
Soil Moisture (NLDAS-2)	1/8° (~12 km)	8 days	cm/cm	Simulated by VIC

2.3. Drought Detection

The root-zone soil moisture percentile is utilized to detect and characterize drought [28,29,72]. The root zone soil moisture percentiles are calculated for each grid in each time step with reference to the period of 1 January 1984 to 31 December 2014. Drought intensity classifications are adopted from the National Drought Mitigation Center (NDMC) of the United States Drought Monitor (USDM), which defines five drought categories as in Table 2.

Table 2. United States Drought Monitor (USDM) drought categories employed in this study to categorize drought intensity.

Category	Description	Percentiles (%)
N	Normal/wet condition	31 to 100
D0	Abnormally dry	21 to 30
D1	Moderate drought	11 to 20
D2	Severe drought	6 to 10
D3	Extreme drought	3 to 5
D4	Exceptional drought	0 to 2

2.4. Drought Recovery Duration

The sensitivity of GPP to drought is well documented and its spatiotemporal patterns can be estimated in several ways [73,74]. GPP, a metric of photosynthetic activity, is used in this study to detect the recovery duration of terrestrial ecosystem after drought episodes. First, the normal GPP threshold, which is the mean GPP over the study period, is calculated for each grid at 8-day time step [75]. Then, the ecosystem recovery from a drought episode is defined when the post-drought GPP reverts and stays above the normal condition (GPP normal threshold) within one-month (4 consecutive 8-day periods) [48,75]. Figure 1 provides a schematic overview of the methodology and analysis of this study.

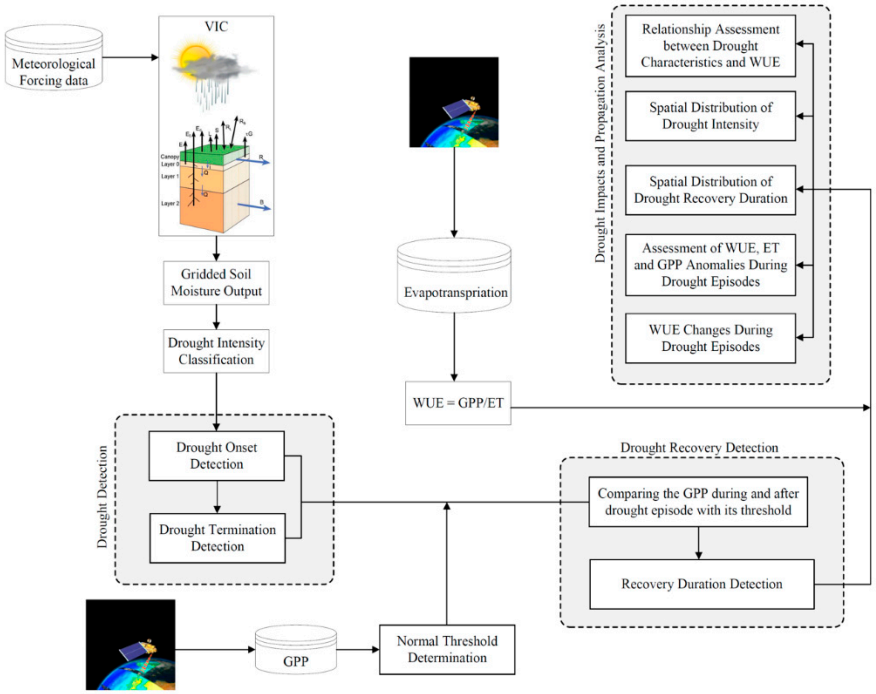

Figure 1. The framework for analyzing terrestrial drought recovery considering Gross Primary Productivity (GPP) and assessing Water Use Efficiency (WUE) response to drought and decomposing the influential factors.

3. Results

The carbon and water cycles have very strong relation and it implies that a disturbance in each component of WUE (i.e., GPP or ET), which can be caused by a hydrological extreme event, may impact the carbon cycle as well. In other words, drought is an intermittent disturbance in the water cycle, which can significantly impact the terrestrial carbon cycle [73,75].

During 2000 to 2014, the average WUE over the Contiguous US (CONUS) is 1.95 gC/kg·H_2O and shows great spatial variations (Figure 2). The dry ecosystems of California, Nevada, Arizona, New Mexico, Utah and west Texas indicate high values of WUE ranging from 2.4 gC/kg·H_2O to 4 gC/kg·H_2O. Whereas, WUE is generally less than 1.6 gC/kg·H_2O in the Midwestern US. At the biome level (shown in Figure 3), EBF and Shrublands show the largest WUE and Cropland and DNF indicate the lowest WUE. According to Figures 2 and 3, arid ecosystems indicate the highest WUE (3.2 gC/kg·H_2O), followed by the coastal regions that show comparable WUE values (2.2 gC/kg·H_2O). The observed differences in WUE among biomes and ecosystems have been well documented by previous studies [3,31,76]. Caused by heterogeneities in both environmental conditions and plant physiological characteristics, the drivers controlling the spatial pattern of WUE are determined by elevation, latitude, plant morphology and climate conditions [61,77].

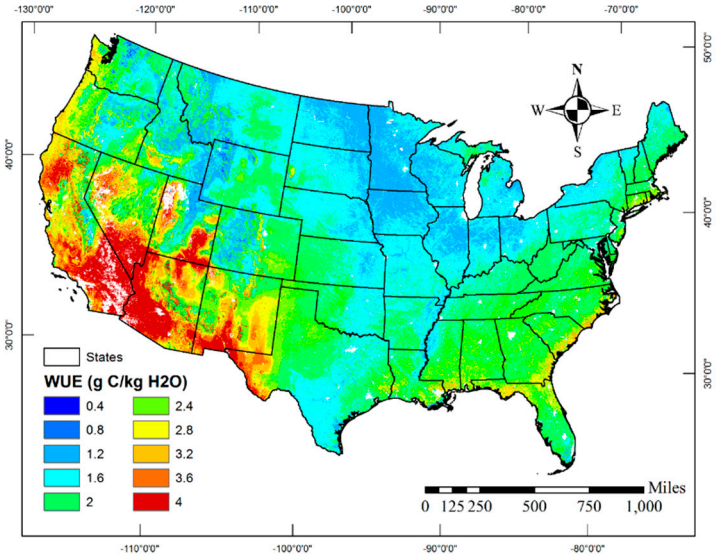

Figure 2. Spatial distribution of mean water use efficiency (WUE) over the contiguous US (CONUS) for the study period (2000–2014).

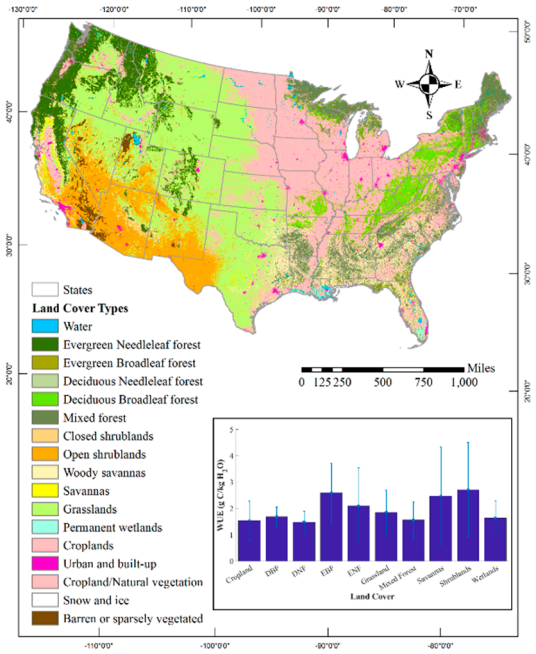

Figure 3. Spatial distribution of land cover over the CONUS and the average WUE of each biome during 2000–2014. The lines indicate ±1 standard deviation for each case.

Figure 4 shows the drought severity and drought recovery duration over the CONUS for 2002, 2008, 2011 and 2012 drought episodes. In 2002, the western US faced more severe drought and some regions in Utah, Colorado, Arizona and southern California and Nevada experienced extreme drought. Accordingly, drought recovery for these regions took longer time and for the regions that experienced extreme drought condition, the minimum drought recovery is found 3 months. On the other hand, eastern US regions (e.g., North and South Carolina and Virginia) experienced severe drought and the drought recovery duration for these regions was relatively shorter. In 2008, the severe and extreme drought extent was less than 2002. California, Wisconsin and Washington were among the states that experienced severe drought in 2008. In California and Washington, the areas that were not covered with cropland biome indicate longer drought recovery. Meanwhile, Wisconsin is covered with more cropland biome and drought recovery was relatively shorter for it in 2008. In North Dakota, Nevada, Utah and Montana, most of which are covered with grasslands, the regions affected by severe drought show longer drought recovery duration.

Additionally, Figure 4 shows that Texas, Oklahoma, Kansas, New Mexico and Arizona faced an extreme drought episode in 2011 [76,77] and the drought recovery duration is found to be over 3–4 months in the region. The 2012 drought was one of the worst drought episodes in recent years which had catastrophic impacts and caused $40 billion damage, mostly due to agricultural losses [78–80]. Almost two-thirds of the nation dealt with drought on September 2012, according to the US Drought Monitor [81]. Figure 4 shows that the central and Midwest states were impacted with severe and extreme drought in 2012. Drought recovery duration is found to be between 2–3 months for most of the region, which is actually a markedly long period, since the drought initiated during the growing season, lasted for several months and then recovered 2–3 months after termination, which might have even affected the following year's harvest and crop yield.

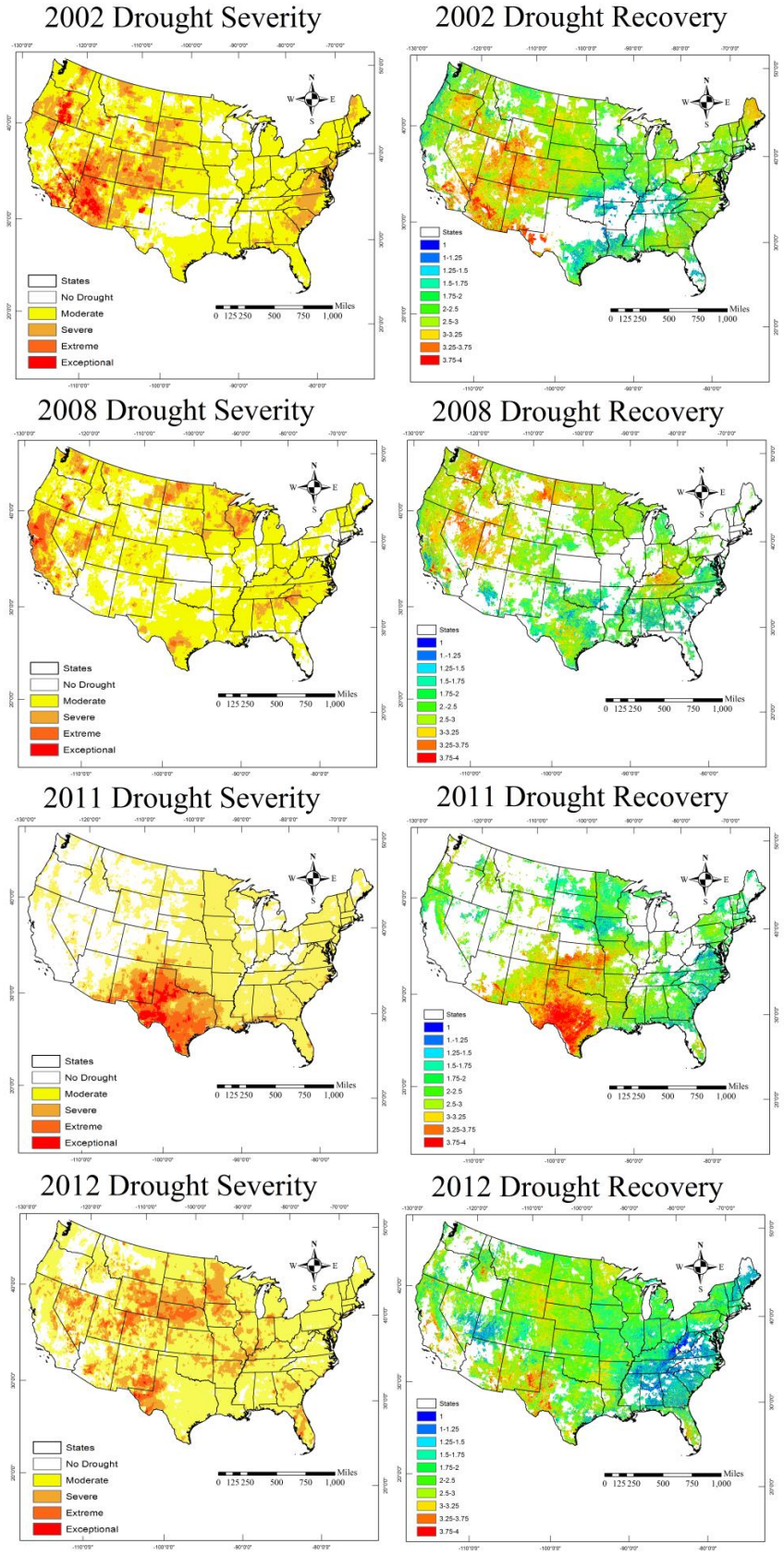

Figure 4. Spatial distribution of drought severity (left) and drought recovery duration (right) for 2002, 2008, 2011 and 2012 drought episodes.

4. Discussion

In order to better understand the terrestrial impacts of drought, the response of water use efficiency (WUE) is investigated for different drought episodes. The range of WUE during drought is from 1 to 7 (g C/kg H_2O), which in the south and southwest shows the maximum. Figure 5 shows WUE anomaly during the four major drought episodes of 2002, 2008, 2011 and 2012 across the CONUS. From the figure, it can be seen that WUE responds differently to various drought events for different biomes and climates. In general, the arid areas which faced severe drought show significant increase in WUE during the drought episodes. This is in agreement with previous studies [30,82] indicating that plants in arid regions are highly adapted to the water scarcity associated with arid climate and have more resiliency to water deficits owing to a series of conservative water-use strategies [77]. Such an adaptation helps the vegetation in arid regions to reduce water loss and maintain vegetation growth. In cold regions, vegetation growth is mainly constrained by air temperature and solar radiation. The higher carbon uptake due to hotter weather that usually coincide with drought episodes [83,84] may increase WUE in these regions [30]. Overall, comparing Figures 4 and 5, WUE is found to substantially increase in response to extreme droughts in each drought episode, indicating that if a region experiences severe drought (or worse), WUE is likely to increase during the drought episode.

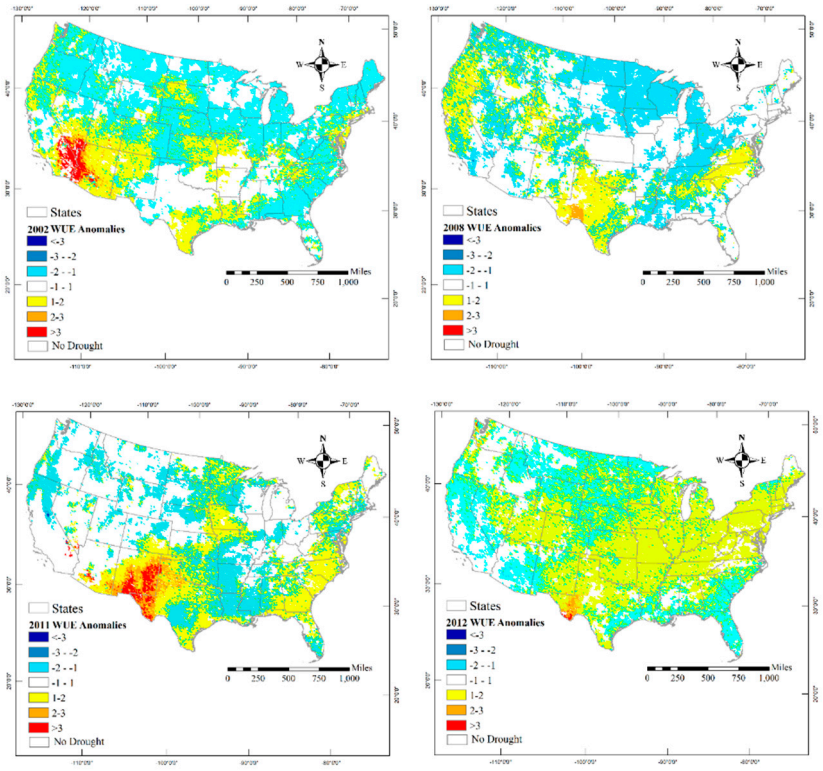

Figure 5. Spatial distribution of WUE anomalies during 2002, 2008, 2011 and 2012 drought episodes.

Figure 6 shows the relation between drought recovery time and drought duration and intensity for 2002, 2008, 2011 and 2012 drought episodes. For each year, the areas affected by drought are considered and the three characteristics are extracted and plotted against each other. For example, in 2012 drought when a region experienced a severe drought for 10 months, the expected drought recovery range was from 2.25 to 2.75 months. In general, a more severe drought episode is expected to result in longer recovery time compared to moderate droughts, which is approved by the results of Figure 6. Additionally, a longer drought episode increases the likelihood of protracted drought recovery. Comparing these four drought episodes reveals that in 2008, the area that experienced prolonged severe drought was relatively less than the other drought episodes and consequently, the affected

regions needed rather shorter recovery time. In 2011, the area affected by a prolonged drought episode shows a wider range of recovery time (compared to other years) and the recovery duration tends to be longer for the regions that experienced more severe droughts. In general, Figure 6 implies that drought duration, recovery and severity are positively correlated, meaning that a prolonged drought will generally result in longer drought recovery time. Similarly, the regions experiencing more severe drought episodes will require more time to recover from drought.

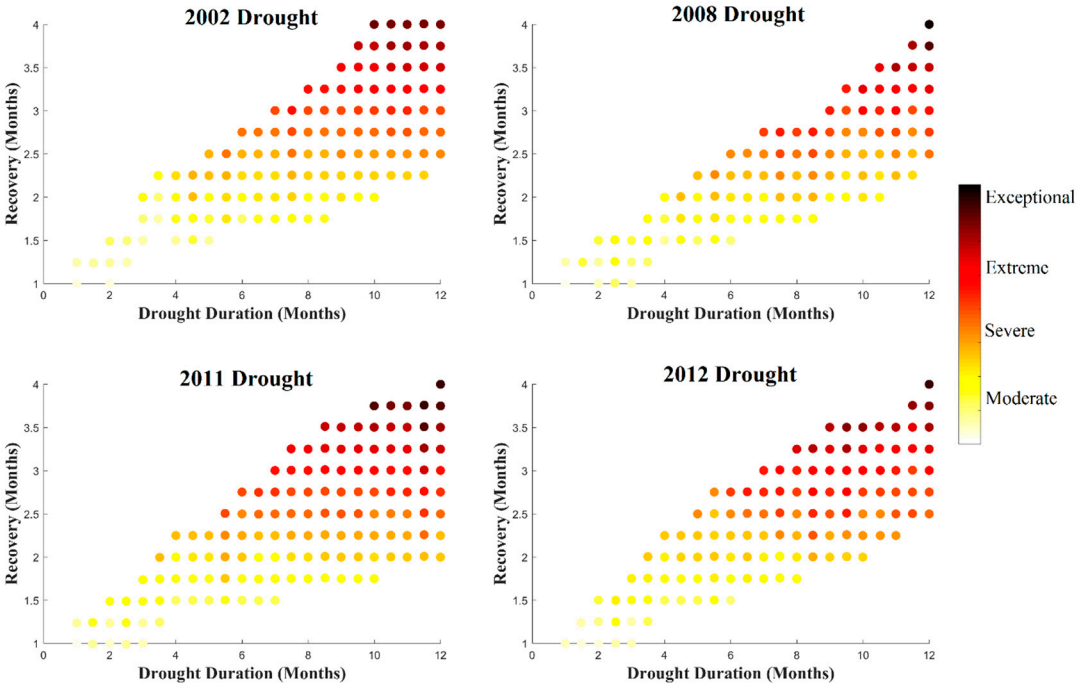

Figure 6. The relation between drought recovery time (y-axis), drought duration (x-axis) and drought intensity (color bar) for the 2002, 2008, 2011 and 2012 drought episodes.

To assess descriptive statistics of WUE changes and to better understand terrestrial response to agricultural drought, the WUE changes are investigated with drought severity. Figure 7 shows the WUE anomaly for each drought severity level for the 2002, 2008, 2011 and 2012 drought episodes over the affected areas. From the figure, a similar pattern can be found for the WUE changes in response to various drought episodes with different severities. In general, WUE shows sharper and higher positive anomalies when a region is affected by a more severe drought. During the 2002 drought episode, the areas affected by extreme or more intense drought showed an increase in WUE with a maximum value of 1.25 gC/kg H_2O. The regions affected by moderate drought in the same year showed relatively lower changes of WUE with the minimum and maximum anomaly of -0.3 and 0.5, respectively. In the 2008 drought episode, more than 75% of the drought affected areas showed a positive anomaly for WUE. Meanwhile, WUE anomaly is almost always (in 93% of areas) positive for severe to extreme droughts. WUE changes in the 2011 drought episode showed wider range and higher maxima compared to other drought episodes. The median of WUE anomaly for the regions affected by severe to extreme drought was 0.5 gC/kg H_2O in 2011. The 2012 drought event showed similar results and more than 75% of the regions affected by drought indicate positive WUE anomaly in 2012. In general, Figure 7 reveals that WUE deviation and drought severity are positively correlated and a more severe drought increases the likelihood of positive WUE anomaly.

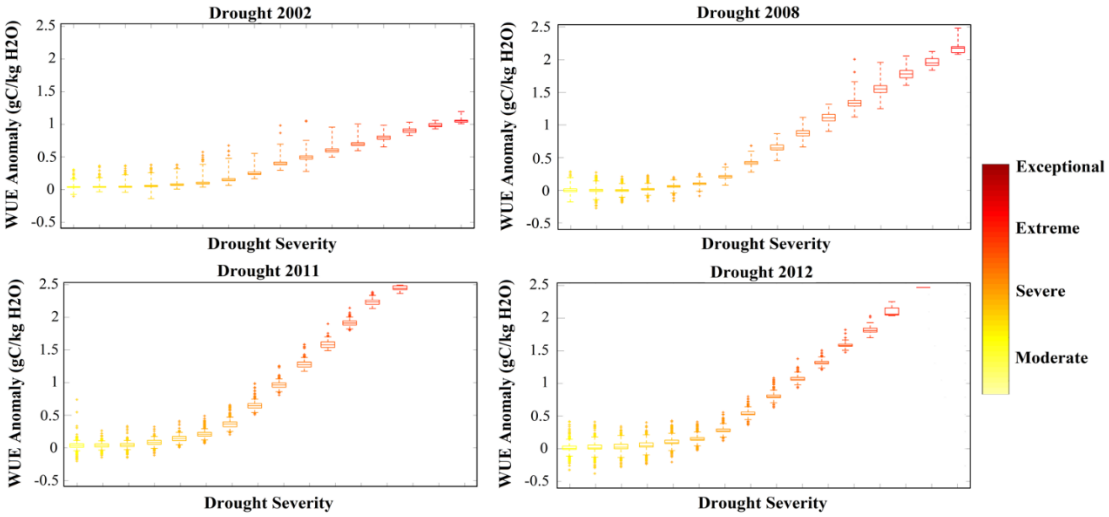

Figure 7. The distribution of WUE anomaly in response to varied drought severities for the 2002, 2008, 2011 and 2012 drought episodes.

To better understand the changes of WUE in relation to its components (ET and GPP), the distribution of relative anomalies of GPP, ET and WUE are plotted in Figure 8 for the 2002, 2008, 2011 and 2012 drought episodes. In the figure, the blue curves on the axes represent the distribution of the corresponding variable. The figure indicates that GPP and ET can have either positive or negative anomalies during drought. However, the distribution diagram reveals that negative anomaly occurs more often (i.e., the distributions are negatively skewed). Comparing the results of different years, WUE anomaly reaches higher values (darker colors) in 2002 and 2011, which can be attributed to higher severity of drought in these years. Previous studies found that drought causes substantial reduction in GPP (about 35% decrease) over most biome land covers, whereas it slightly enhances GPP (about 7% increase) in evergreen broadleaf forests and shrublands [75,85]. In North America, a large reduction of GPP (over 50%) was found resulting in 51% decrease of net carbon uptake during the 2000–2004 drought in western North America [86–88]. Similarly, studies found decreasing (ranging from 1% to 28%) and increasing (ranging from 7% to 15%) WUE under drought stress, for different drought severities and land covers [1,2,86]. Overall, decomposing WUE in relation to its components in Figure 8 reveals that if the relative anomaly of ET is larger than that of GPP, WUE anomaly will be positive (shown in green color), whereas if GPP is higher than ET (lower half of the plot, shown in brown color), WUE anomaly will be negative.

Evapotranspiration (ET) is an essential component of energy and water cycles and it is influential in multitude of earth processes, subsequently affecting meteorology and agriculture [88,89]. Several studies have shown the role of evapotranspiration in developing and intensifying droughts [90,91]. In some studies, potential evapotranspiration anomaly has been merely utilized as a measure of drought intensity and as a means for predicting drought [92]. To better understand the terrestrial impacts of drought on evapotranspiration (ET), the changes of ET are investigated for different drought episodes. Figure 9 shows the ET anomaly during the four major drought episodes of 2002, 2008, 2011 and 2012 across the CONUS. From the figure, it can be seen that ET tends to be below average in the areas affected by severe (or more intense) drought. This negative anomaly is found to be common in both dry and humid climates, which highlights that water availability is the dominant factor for evapotranspiration deviation [1,93]. The highest changes of ET is found during the 2011 Texas drought, reducing ET about 100–200 mm. Evapotranspiration consists of three components: interception, soil surface evaporation and transpiration. Further study can shed light on different responses of evaporation and transpiration over different land covers during drought.

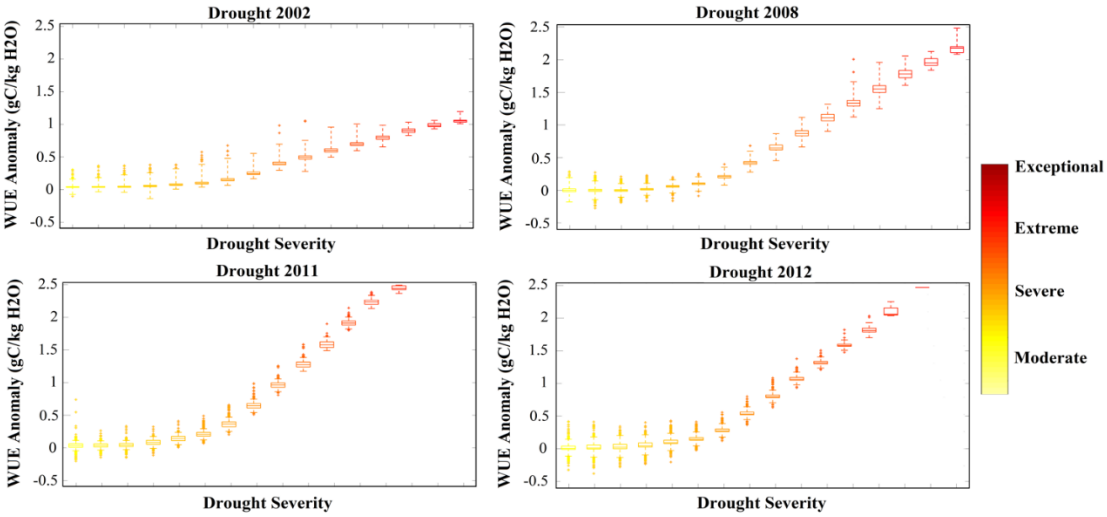

Figure 8. The distribution of relative anomaly of evapotranspiration (ET), GPP and WUE for the 2002, 2008, 2011 and 2012 drought episodes. In each plot, the blue curves on the axes show the distribution of the corresponding variable.

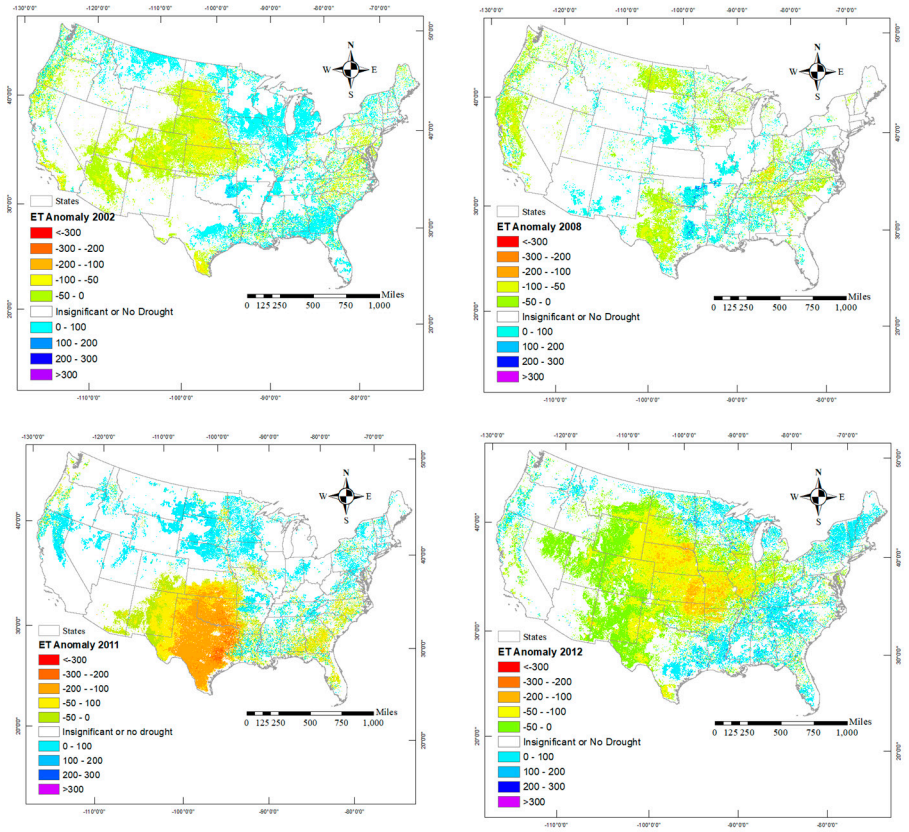

Figure 9. Spatial distribution of ET anomalies (mm) for the 2002, 2008, 2011 and 2012 drought episodes.

Drought episodes usually start with rainfall deficiency, which leads to reduced soil moisture and it is often assumed that ET decreases when soil moisture decreases. On the other hand, it has been discussed that ET is restricted to low values of available soil moisture [94,95]. Therefore, for different soil moisture content, ET will change based on the variability in atmospheric conditions rather than the variability of soil moisture. In humid climates which are generally energy limited, during drought, atmospheric conditions intensify ET and lead to increased ET [95]. Similarly, in water limited dry

climates, positive ET anomalies have been observed during warm conditions that often coincide with drought [40,93,94,96]. The deep and extensive root systems of plants can obtain water from lower levels of soil column near the water table rather than the smaller top layers of soil zone, which may increase the transpiration and consequently increase ET during drought [40,93].

Drought can cause a wide range of impacts on terrestrial ecosystems, including influence the vegetation physiology, phenology, growth, pest outbreak and fire occurrence [1,97]. In this study, we evaluated drought impacts focusing on the changes of soil moisture and ecosystem water use efficiency during the 15 years of 2002–2014 over the CONUS. Using fine spatial and temporal resolution remotely sensed data and model simulations, we were able to quantify the impacts with high resolution and significant meaningful patterns were extracted. The results of this study confirmed certain previous findings, such as increase in WUE and significant decrease in GPP and ET during severe drought. This study showed that the increase rate of WUE is directly related to drought severity and for a severe or extreme drought episode, there is a high likelihood of increasing WUE. Moreover, this study investigated terrestrial drought recovery based on GPP variations and concluded that drought recovery is positively correlated with drought severity and drought duration. These positive correlations shed light on the understanding of the response of terrestrial ecosystems to drought and their importance for forecasting ecosystem dynamics in future climate scenarios. The findings of this study highlighted the substantial impacts that drought can have on the ecosystem, which implies the necessity of advancing drought forecasting methods and incorporating proactive drought risk management strategies in order to mitigate such environmental risks. This study investigated the recovery duration over the CONUS after agricultural drought using GPP, which has never been investigated. Additionally, results showed that WUE increases in the regions that experienced severe or worse drought condition.

5. Summary and Conclusions

This study investigated the agricultural drought impacts on water use efficiency (WUE) and its components; gross primary productivity (GPP) and evapotranspiration (ET), as well as the recovery duration that terrestrial ecosystems require to revert to pre-drought normal conditions. WUE was analyzed for different land cover types and arid and coastal ecosystems indicated the highest WUE and Midwest US was associated with the lowest WUE. Drought recovery was analyzed according to the GPP rate and it revealed that the required time for each region to revert to its pre-drought condition is positively correlated with drought severity. Therefore, a more severe drought will most likely result in a longer drought recovery time. Additionally, a prolonged drought episode increases the likelihood of protracted drought recovery. During drought, WUE showed a tendency to increase in response to extreme drought condition. Decomposing WUE anomalies to its components during drought illustrated that if the relative anomaly of ET is larger than that of GPP, WUE anomaly will be positive and if the relative anomaly of ET is smaller than that of GPP, WUE anomaly will be negative. Moreover, the spatial distribution of ET anomaly showed that ET has a tendency to be below average in the regions affected by severe (or more intense) and prolonged drought in both dry and humid climates, corroborating the dominance of water availability on evapotranspiration.

Author Contributions: B.A., A.A., G.T. and H.M. conceived the research idea; B.A. processed the data; B.A. and A.A. analyzed the results. All the authors contributed to the manuscript.

Funding: This research was partially funded by NOAA grant NA18OAR4310319.

Acknowledgments: The MODIS evapotranspiration and gross primary productivity data were obtained from the Numerical Terradynamic Simulation Group at University of Montana (http://www.ntsg.umt.edu). Additionally, the MODIS biome land cover types were acquired from the global land cover facility of the University of Maryland (http://glcf.umd.edu/data/lc/).

Conflicts of Interest: The authors declare no conflict of interest.

References

1. Huang, L.; He, B.; Han, L.; Liu, J.; Wang, H.; Chen, Z. A global examination of the response of ecosystem water-use efficiency to drought based on MODIS data. *Sci. Total Environ.* **2017**, *601–602*, 1097–1107. [CrossRef] [PubMed]
2. Yu, Z.; Wang, J.; Liu, S.; Rentch, J.S.; Sun, P.; Lu, C. Global gross primary productivity and water use efficiency changes under drought stress. *Environ. Res. Lett.* **2017**, *12*, 014016. [CrossRef]
3. Yang, Y.; Guan, H.; Batelaan, O.; Mcvicar, T.R.; Long, D.; Piao, S.; Liang, W.; Liu, B.; Jin, Z.; Simmons, C.T. Contrasting responses of water use efficiency to drought across global terrestrial ecosystems. *Sci. Rep.* **2016**, *6*, 23284. [CrossRef] [PubMed]
4. Karamouz, M.; Yazdi, M.S.; Ahmadi, B.; Zahraie, B. A System Dynamics Approach to Economic Assessment of Water Supply and Demand Strategies. In Proceedings of the World Environmental and Water Resources Congress 2011, Palm Springs, CA, USA, 22–26 May 2011.
5. IPCC. *Climate Change 2014—Impacts, Adaptation and Vulnerability: Regional Aspects*; Cambridge University Press: New York, NY, USA, 2014; ISBN 1107058163.
6. Zeng, N.; Qian, H.; Munoz, E.; Iacono, R. How strong is carbon cycle-climate feedback under global warming? *Geophys. Res. Lett.* **2004**, *31*, 5. [CrossRef]
7. Karamouz, M.; Ahmadi, A.; Semsar, Y.M.S.; Ahmadi, B. Economic Assessment of Water Resources Management Strategies. *J. Irrig. Drain. Eng.* **2014**, *140*, 4013005. [CrossRef]
8. Ahmadalipour, A.; Moradkhani, H.; Svoboda, M. Centennial drought outlook over the CONUS using NASA-NEX downscaled climate ensemble. *Int. J. Climatol.* **2016**, *37*, 2477–2491. [CrossRef]
9. Karamouz, M.; Ahmadi, B.; Zahmatkesh, Z. Developing an Agricultural Planning Model in a Watershed Considering Climate Change Impacts. *J. Water Resour. Plan. Manag.* **2013**, *139*, 349–363. [CrossRef]
10. Irannezhad, M.; Ahmadi, B.; Kløve, B.; Moradkhani, H. Atmospheric circulation patterns explaining climatological drought dynamics in the boreal environment of Finland, 1962–2011. *Int. J. Climatol.* **2017**, *37*, 801–817. [CrossRef]
11. Ahmadi, B.; Ahmadalipour, A.; Moradkhani, H. Hydrological drought persistence and recovery over the CONUS: A multi-stage framework considering water quantity and quality. *Water Res.* **2019**, *150*, 97–110. [CrossRef]
12. Keyantash, J.; Dracup, J.A. The Quantification of Drought: An Evaluation of Drought Indices. *Bull. Am. Meteorol. Soc.* **2002**, *83*, 1167–1180. [CrossRef]
13. Sheffield, J.; Wood, E.F. Global Trends and Variability in Soil Moisture and Drought Characteristics, 1950–2000, from Observation-Driven Simulations of the Terrestrial Hydrologic Cycle. *J. Clim.* **2008**, *21*, 432–458. [CrossRef]
14. Mishra, A.; Vu, T.; Veettil, A.V.; Entekhabi, D. Drought monitoring with soil moisture active passive (SMAP) measurements. *J. Hydrol.* **2017**, *552*, 620–632. [CrossRef]
15. Vereecken, H.; Huisman, J.A.; Bogena, H.; Vanderborght, J.; Vrugt, J.A.; Hopmans, J.W. On the value of soil moisture measurements in vadose zone hydrology: A review. *Water Resour. Res.* **2008**, *44*, W00D06. [CrossRef]
16. Escorihuela, M.J.; Quintana-Seguí, P. Comparison of remote sensing and simulated soil moisture datasets in Mediterranean landscapes. *Remote Sens. Environ.* **2016**, *180*, 99–114. [CrossRef]
17. Narasimhan, B.; Srinivasan, R. Development and evaluation of Soil Moisture Deficit Index (SMDI) and Evapotranspiration Deficit Index (ETDI) for agricultural drought monitoring. *Agric. For. Meteorol.* **2005**, *133*, 69–88. [CrossRef]
18. Ceppi, P.; Zelinka, M.D.; Hartmann, D.L. The response of the Southern Hemispheric eddy-driven jet to future changes in shortwave radiation in CMIP5. *Geophys. Res. Lett.* **2014**, *41*, 3244–3250. [CrossRef]
19. Qin, Y.; Yang, D.; Lei, H.; Xu, K.; Xu, X. Comparative analysis of drought based on precipitation and soil moisture indices in Haihe basin of North China during the period of 1960–2010. *J. Hydrol.* **2015**, *526*, 55–67. [CrossRef]
20. Ahmadalipour, A.; Moradkhani, H.; Yan, H.; Zarekarizi, M. Remote Sensing of Drought: Vegetation, Soil Moisture, and Data Assimilation BT. In *Remote Sensing of Hydrological Extremes*; Lakshmi, V., Ed.; Springer International Publishing: Cham, Switzerland, 2017; pp. 121–149, ISBN 978-3-319-43744-6.

21. Rebel, K.T.; de Jeu, R.A.M.; Ciais, P.; Viovy, N.; Piao, S.L.; Kiely, G.; Dolman, A.J. A global analysis of soil moisture derived from satellite observations and a land surface model. *Hydrol. Earth Syst. Sci.* **2012**, *16*, 833–847. [CrossRef]
22. Xu, X.; Li, J.; Tolson, B.A. Progress in integrating remote sensing data and hydrologic modeling. *Prog. Phys. Geogr. Earth Environ.* **2014**, *38*, 464–498. [CrossRef]
23. Champagne, C.; McNairn, H.; Berg, A.A. Monitoring agricultural soil moisture extremes in Canada using passive microwave remote sensing. *Remote Sens. Environ.* **2011**, *115*, 2434–2444. [CrossRef]
24. Kang, C.S.; Kanniah, K.D.; Kerr, Y.H.; Cracknell, A.P. Analysis of in-situ soil moisture data and validation of SMOS soil moisture products at selected agricultural sites over a tropical region. *Int. J. Remote Sens.* **2016**, *37*, 3636–3654. [CrossRef]
25. Martínez-Fernández, J.; González-Zamora, Á.; Sanchez, N.; Gumuzzio, A.; Herrero-Jiménez, C. Satellite soil moisture for agricultural drought monitoring: Assessment of the SMOS derived Soil Water Deficit Index. *Remote Sens. Environ.* **2016**, *177*, 277–286. [CrossRef]
26. Wagner, W.; Scipal, K.; Pathe, C.; Gerten, D.; Lucht, W.; Rudolf, B. Evaluation of the agreement between the first global remotely sensed soil moisture data with model and precipitation data. *J. Geophys. Res. Atmos.* **2003**, *108*. [CrossRef]
27. Liu, Y.Y.; Parinussa, R.M.; Dorigo, W.A.; De Jeu, R.A.M.; Wagner, W.; van Dijk, A.I.J.M.; McCabe, M.F.; Evans, J.P. Developing an improved soil moisture dataset by blending passive and active microwave satellite-based retrievals. *Hydrol. Earth Syst. Sci.* **2011**, *15*, 425–436. [CrossRef]
28. Yan, H.; Zarekarizi, M.; Moradkhani, H. Toward improving drought monitoring using the remotely sensed soil moisture assimilation: A parallel particle filtering framework. *Remote Sens. Environ.* **2018**, *216*, 456–471. [CrossRef]
29. Yan, H.; Moradkhani, H.; Zarekarizi, M. A probabilistic drought forecasting framework: A combined dynamical and statistical approach. *J. Hydrol.* **2017**, *548*, 291–304. [CrossRef]
30. Liu, Y.; Xiao, J.; Ju, W.; Zhou, Y.; Wang, S.; Wu, X. Water use efficiency of China's terrestrial ecosystems and responses to drought. *Sci. Rep.* **2015**, *5*, 13799. [CrossRef]
31. Tang, X.; Li, H.; Desai, A.R.; Nagy, Z.; Luo, J.; Kolb, T.E.; Olioso, A.; Xu, X.; Yao, L.; Kutsch, W.; et al. How is water-use efficiency of terrestrial ecosystems distributed and changing on Earth? *Sci. Rep.* **2014**, *4*, 7483. [CrossRef] [PubMed]
32. Yang, F.; Ichii, K.; White, M.A.; Hashimoto, H. Developing a continental-scale measure of gross primary production by combining MODIS and AmeriFlux data through Support Vector Machine approach. *Remote Sens. Environ.* **2007**, *110*, 109–122. [CrossRef]
33. He, M.; Kimball, J.S.; Running, S.; Ballantyne, A.; Guan, K.; Huemmrich, F. Remote Sensing of Environment Satellite detection of soil moisture related water stress impacts on ecosystem productivity using the MODIS-based photochemical re fl ectance index. *Remote Sens. Environ.* **2016**, *186*, 173–183. [CrossRef]
34. Lawrence, D.M.; Thornton, P.E.; Oleson, K.W.; Bonan, G.B. The Partitioning of Evapotranspiration into Transpiration, Soil Evaporation, and Canopy Evaporation in a GCM: Impacts on Land–Atmosphere Interaction. *J. Hydrometeorol.* **2007**, *8*, 862–880. [CrossRef]
35. Zhang, X.; Moran, M.S.; Zhao, X.; Liu, S.; Zhou, T.; Ponce-Campos, G.E.; Liu, F. Remote Sensing of Environment Impact of prolonged drought on rainfall use ef fi ciency using MODIS data across China in the early 21st century. *Remote Sens. Environ.* **2014**, *150*, 188–197. [CrossRef]
36. Ponce-Campos, G.E.; Moran, M.S.; Huete, A.; Zhang, Y.; Bresloff, C.; Huxman, T.E.; Eamus, D.; Bosch, D.D.; Buda, A.R.; Gunter, S.A.; et al. Ecosystem resilience despite large-scale altered hydroclimatic conditions. *Nature* **2013**, *494*, 349–352. [CrossRef] [PubMed]
37. Tang, X.; Li, H.; Xu, X.; Luo, J.; Li, X.; Ding, Z.; Xie, J. Potential of MODIS data to track the variability in ecosystem water-use efficiency of temperate deciduous forests. *Ecol. Eng.* **2016**, *91*, 381–391. [CrossRef]
38. Mazdiyasni, O.; Aghakouchak, A. Substantial increase in concurrent droughts and heatwaves in the United States. *Proc. Natl. Acad. Sci. USA* **2015**, *112*, 11484–11489. [CrossRef]
39. Chiang, F.; Mazdiyasni, O.; Aghakouchak, A. Amplified warming of droughts in southern United States in observations and model simulations. *Sci. Adv.* **2018**, *4*, eaat2380. [CrossRef]
40. Teuling, A.J.; Van Loon, A.F.; Seneviratne, S.I.; Lehner, I.; Aubinet, M.; Heinesch, B.; Bernhofer, C.; Grünwald, T.; Prasse, H.; Spank, U. Evapotranspiration ampli fi es European summer drought. *Geophys. Res. Lett.* **2015**, *40*, 2071–2075. [CrossRef]

41. Huntington, T. Evidence for Intensification of the Global Water Cycle: Review and Synthesis. *J. Hydrol.* **2006**, *319*, 83–95. [CrossRef]
42. Dan, L.I.U.; Chenglong, Y.U.; Fang, Z. Response of the water use efficiency of natural vegetation to drought in Northeast China. *J. Geogr. Sci.* **2018**, *28*, 611–628.
43. Pan, M.; Yuan, X.; Wood, E.F. A probabilistic framework for assessing drought recovery. *Geophys. Res. Lett.* **2013**, *40*, 3637–3642. [CrossRef]
44. Dechant, C.M.; Moradkhani, H. Analyzing the sensitivity of drought recovery forecasts to land surface initial conditions. *J. Hydrol.* **2015**, *526*, 89–100. [CrossRef]
45. Secchi, F.; Zwieniecki, M.A. Down-Regulation of Plasma Intrinsic Protein1 Aquaporin in Poplar Trees Is Detrimental to Recovery from Embolism. *Plant Physiol.* **2014**, *164*, 1789–1799. [CrossRef] [PubMed]
46. Martorell, S.; Diaz-espejo, A.; Medrano, H.; Ball, M.C.; Choat, B. Rapid hydraulic recovery in Eucalyptus pauciflora after drought: Linkages between stem hydraulics and leaf gas exchange. *Plant Cell Environ.* **2014**, *37*, 617–626. [CrossRef] [PubMed]
47. Parry, S.; Prudhomme, C.; Wilby, R.L.; Wood, P.J. Drought termination: Concept and characterisation. *Prog. Phys. Geogr.* **2016**, *40*, 743–767. [CrossRef]
48. Schwalm, C.R.; Anderegg, W.R.L.; Michalak, A.M.; Fisher, J.B.; Biondi, F.; Koch, G.; Litvak, M.; Ogle, K.; Shaw, J.D.; Wolf, A.; et al. Global patterns of drought recovery. *Nature* **2017**, *548*, 202–205. [CrossRef] [PubMed]
49. Connor, J.D.; Crossman, N.D.; Banerjee, O.; Bark, R.; Connor, J.; Crossman, N.D. An ecosystem services approach to estimating economic losses associated with drought an ecosystem services approach to estimating economic losses associated with drought. *Ecol. Econ.* **2013**, *91*, 19–27.
50. Nepstad, D.C.; Stickler, C.M.; Soares-filho, B.; Merry, F.; Nin, E. Interactions among Amazon land use, forests and climate: Prospects for a near-term forest tipping point. *Philos. Trans. R. Soc. B Biol. Sci.* **2008**, *363*, 1737–1746. [CrossRef]
51. Running, S.W.; Nemani, R.R.; Heinsch, F.A.N.N.; Zhao, M.; Reeves, M.; Hashimoto, H.A. Continuous Satellite-Derived Measure of Global Terrestrial Primary Production. *Bioscience* **2004**, *54*, 547–560. [CrossRef]
52. Zhao, M.; Heinsch, F.A.; Nemani, R.R.; Running, S.W. Improvements of the MODIS terrestrial gross and net primary production global data set. *Remote Sens. Environ.* **2005**, *95*, 164–176. [CrossRef]
53. Mu, Q.; Heinsch, F.A.; Zhao, M.; Running, S.W. Development of a global evapotranspiration algorithm based on MODIS and global meteorology data. *Remote Sens. Environ.* **2007**, *111*, 519–536. [CrossRef]
54. Mu, Q.; Zhao, M.; Running, S.W. Improvements to a MODIS global terrestrial evapotranspiration algorithm. *Remote Sens. Environ.* **2011**, *115*, 1781–1800. [CrossRef]
55. Heinsch, F.; Reeves, M.; Votava, P.; Kang, S.; Cristina, M.; Zhao, M.; Glassy, J.; Jolly, W.; Loehman, R.; Bowker, C.F.; et al. *User's Guide GPP and NPP (MOD17A2/A3) Products NASA MODIS Land Algorithm*; The University of Montana: Missoula, MT, USA, 2003.
56. Cohen, W.B.; Maiersperger, T.K.; Turner, D.P.; Ritts, W.D.; Pflugmacher, D.; Kennedy, R.E.; Kirschbaum, A.; Running, S.W.; Costa, M.; Gower, S.T. MODIS land cover and LAI collection 4 product quality across nine sites in the western hemisphere. *IEEE Trans. Geosci. Remote Sens.* **2006**, *44*, 1843–1857. [CrossRef]
57. Heinsch, F.A.; Zhao, M.; Running, S.W.; Kimball, J.S.; Nemani, R.R.; Davis, K.J.; Bolstad, P.V.; Cook, B.D.; Desai, A.R.; Ricciuto, D.M.; et al. Evaluation of Remote Sensing Based Terrestrial Productivity from MODIS Using Regional Tower Eddy Flux Network Observations. *IEEE Trans. Geosci. Remote Sens.* **2006**, *44*, 1908–1925. [CrossRef]
58. Turner, D.P.; Ritts, W.D.; Cohen, W.B.; Gower, S.T.; Running, S.W.; Zhao, M.; Costa, M.H.; Kirschbaum, A.A.; Ham, J.M.; Saleska, S.R.; et al. Evaluation of MODIS NPP and GPP products across multiple biomes. *Remote Sens. Environ.* **2006**, *102*, 282–292. [CrossRef]
59. Zargar, A.; Sadiq, R.; Naser, B.; Khan, F.I. A review of drought indices. *Environ. Rev.* **2011**, *19*, 333–349. [CrossRef]
60. Xiao, J.; Zhuang, Q.; Law, B.E.; Chen, J.; Baldocchi, D.D.; Cook, D.R.; Oren, R.; Richardson, A.D.; Wharton, S.; Ma, S.; et al. Remote Sensing of Environment A continuous measure of gross primary production for the conterminous United States derived from MODIS and AmeriFlux data. *Remote Sens. Environ.* **2010**, *114*, 576–591. [CrossRef]
61. Xue, B.-L.; Guo, Q.; Otto, A.; Xiao, J.; Tao, S.; Li, L. Global patterns, trends, and drivers of water use efficiency from 2000 to 2013. *Ecosphere* **2015**, *6*, art174. [CrossRef]

62. Zhang, K.; Kimball, J.S.; Running, S.W. A review of remote sensing based actual evapotranspiration estimation. *Wiley Interdiscip. Rev. Water* **2016**, *3*, 834–853. [CrossRef]
63. Wolf, S.; Keenan, T.F.; Fisher, J.B.; Baldocchi, D.D.; Desai, A.R.; Richardson, A.D.; Scott, R.L.; Law, B.E.; Litvak, M.E.; Brunsell, N.A.; et al. Warm spring reduced carbon cycle impact of the 2012 US summer drought. *Proc. Natl. Acad. Sci. USA* **2016**, *113*, 5880–5885. [CrossRef]
64. Zscheischler, J.; Mahecha, M.D.; von Buttlar, J.; Harmeling, S.; Jung, M.; Rammig, A.; Randerson, J.T.; Schölkopf, B.; Seneviratne, S.I.; Tomelleri, E.; et al. A few extreme events dominate global interannual variability in gross primary production. *Environ. Res. Lett.* **2014**, *9*, 35001. [CrossRef]
65. Mu, Q.; Zhao, M.; Running, S.W. *Numerical Terradynamic Simulation Group MODIS Global Terrestrial Evapotranspiration (ET) Product (NASA MOD16A2/A3) Collection 5. NASA Headquarters*; Numerical Terradynamic Simulation Group Publications: Missoula, MT, USA, 2013.
66. Velpuri, N.M.; Senay, G.B.; Singh, R.K.; Bohms, S.; Verdin, J.P. A comprehensive evaluation of two MODIS evapotranspiration products over the conterminous United States: Using point and gridded FLUXNET and water balance ET. *Remote Sens. Environ.* **2013**, *139*, 35–49. [CrossRef]
67. Xia, Y.; Mitchell, K.; Ek, M.; Cosgrove, B.; Sheffield, J.; Luo, L.; Alonge, C.; Wei, H.; Meng, J.; Livneh, B.; et al. Continental-scale water and energy flux analysis and validation for North American Land Data Assimilation System project phase 2 (NLDAS-2): 2. Validation of model-simulated streamflow. *J. Geophys. Res. Atmos.* **2012**, *117*. [CrossRef]
68. Liang, X.; Lettenmaier, D.P.; Wood, E.F.; Burges, S.J. A simple hydrologically based model of land surface water and energy fluxes for general circulation models. *J. Geophys. Res. Atmos.* **1994**, *99*, 14415–14428. [CrossRef]
69. Wood, E.F.; Lettenmaier, D.; Liang, X.; Nijssen, B.; Wetzel, S.W. Hydrological modeling of continental-scale basins. *Annu. Rev. Earth Planet. Sci.* **1997**, *25*, 279–300. [CrossRef]
70. Maurer, E.P.; Wood, A.W.; Adam, J.C.; Lettenmaier, D.P.; Nijssen, B. A Long-Term Hydrologically Based Dataset of Land Surface Fluxes and States for the Conterminous United States. *J. Clim.* **2002**, *15*, 3237–3251. [CrossRef]
71. Livneh, B.; Rosenberg, E.A.; Lin, C.; Nijssen, B.; Mishra, V.; Andreadis, K.M.; Maurer, E.P.; Lettenmaier, D.P. A Long-Term Hydrologically Based Dataset of Land Surface Fluxes and States for the Conterminous United States: Update and Extensions. *J. Clim.* **2013**, *26*, 9384–9392. [CrossRef]
72. Shukla, S.; Steinemann, A.C.; Lettenmaier, D.P. Drought Monitoring for Washington State: Indicators and Applications. *J. Hydrometeorol.* **2011**, *12*, 66–83. [CrossRef]
73. Zhao, M.; Running, S.W. Drought-Induced Reduction in Global Terrestrial Net Primary Production from 2000 through 2009. *Science* **2010**, *329*, 940–943. [CrossRef]
74. Beer, C.; Reichstein, M.; Tomelleri, E.; Ciais, P.; Jung, M.; Carvalhais, N.; Rödenbeck, C.; Arain, M.A.; Baldocchi, D.; Bonan, G.B.; et al. Terrestrial Gross Carbon Dioxide Uptake: Global Distribution and Covariation with Climate. *Science* **2010**, *329*, 834–838. [CrossRef] [PubMed]
75. Breshears, D.D.; Cobb, N.S.; Rich, P.M.; Price, K.P.; Allen, C.D.; Balice, R.G.; Romme, W.H.; Kastens, J.H.; Floyd, M.L.; Belnap, J.; et al. Regional vegetation die-off in response to global-change-type drought. *Proc. Natl. Acad. Sci. USA* **2005**, *102*, 15144–15148. [CrossRef]
76. Seager, R.; Goddard, L.; Nakamura, J.; Henderson, N.; Lee, D.E. Dynamical Causes of the 2010/11 Texas–Northern Mexico Drought. *J. Hydrometeorol.* **2013**, *15*, 39–68. [CrossRef]
77. Long, D.; Scanlon, B.R.; Longuevergne, L.; Sun, A.Y.; Fernando, D.N.; Save, H. GRACE satellite monitoring of large depletion in water storage in response to the 2011 drought in Texas. *Geophys. Res. Lett.* **2013**, *40*, 3395–3401. [CrossRef]
78. Rippey, B.R. The U.S. drought of 2012. *Weather Clim. Extrem.* **2015**, *10*, 57–64. [CrossRef]
79. Hoerling, M.; Eischeid, J.; Kumar, A.; Leung, R.; Mariotti, A.; Mo, K.; Schubert, S.; Seager, R. Causes and Predictability of the 2012 Great Plains Drought. *Bull. Am. Meteorol. Soc.* **2013**, *95*, 269–282. [CrossRef]
80. Wang, H.; Schubert, S.; Koster, R.; Ham, Y.-G.; Suarez, M. On the Role of SST Forcing in the 2011 and 2012 Extreme U.S. Heat and Drought: A Study in Contrasts. *J. Hydrometeorol.* **2014**, *15*, 1255–1273. [CrossRef]
81. Otkin, J.A.; Svoboda, M.; Hunt, E.D.; Ford, T.W.; Anderson, M.C.; Hain, C.; Basara, J.B. Flash Droughts: A Review and Assessment of the Challenges Imposed by Rapid-Onset Droughts in the United States. *Bull. Am. Meteorol. Soc.* **2017**, *99*, 911–919. [CrossRef]

82. Vicente-Serrano, S.M.; Gouveia, C.; Camarero, J.J.; Begueria, S.; Trigo, R.; López-Moreno, J.I.; Azorin-Molina, C.; Pasho, E.; Lorenzo-Lacruz, J.; Revuelto, J.; et al. Response of vegetation to drought time-scales across global land biomes. *Proc. Natl. Acad. Sci. USA* **2013**, *110*, 52–57. [CrossRef]
83. Schwingshackl, C.; Hirschi, M.; Seneviratne, S.I. Quantifying Spatiotemporal Variations of Soil Moisture Control on Surface Energy Balance and Near-Surface Air Temperature. *J. Clim.* **2017**, *30*, 7105–7124. [CrossRef]
84. Haghighi, E.; Short Gianotti, D.J.; Akbar, R.; Salvucci, G.D.; Entekhabi, D. Soil and Atmospheric Controls on the Land Surface Energy Balance: A Generalized Framework for Distinguishing Moisture-Limited and Energy-Limited Evaporation Regimes. *Water Resour. Res.* **2018**, *54*, 1831–1851. [CrossRef]
85. Frank, D.; Reichstein, M.; Bahn, M.; Thonicke, K.; Frank, D.; Mahecha, M.D.; Smith, P.; Velde, M.; Vicca, S.; Babst, F.; et al. Effects of climate extremes on the terrestrial carbon cycle: Concepts, processes and potential future impacts. *Glob. Chang. Biol.* **2015**, *21*, 2861–2880. [CrossRef] [PubMed]
86. Schwalm, C.R.; Williams, C.A.; Schaefer, K.; Baldocchi, D.; Black, T.A.; Goldstein, A.H.; Law, B.E.; Oechel, W.C.; Paw, K.T.; Scott, R.L. Reduction in carbon uptake during turn of the century drought in western North America. *Nat. Geosci.* **2012**, *5*, 551–556. [CrossRef]
87. Liao, C.; Zhuang, Q. Reduction of Global Plant Production due to Droughts from 2001 to 2010: An Analysis with a Process-Based Global Terrestrial Ecosystem Model. *Earth Interact.* **2015**, *19*, 1–21. [CrossRef]
88. Rodell, M.; Beaudoing, H.K.; L'Ecuyer, T.S.; Olson, W.S.; Famiglietti, J.S.; Houser, P.R.; Adler, R.; Bosilovich, M.G.; Clayson, C.A.; Chambers, D.; et al. The Observed State of the Water Cycle in the Early Twenty-First Century. *J. Clim.* **2015**, *28*, 8289–8318. [CrossRef]
89. L'Ecuyer, T.S.; Beaudoing, H.K.; Rodell, M.; Olson, W.; Lin, B.; Kato, S.; Clayson, C.A.; Wood, E.; Sheffield, J.; Adler, R. The observed state of the energy budget in the early twenty-first century. *J. Clim.* **2015**, *28*, 8319–8346. [CrossRef]
90. Ford, T.W.; Labosier, C.F. Meteorological conditions associated with the onset of flash drought in the Eastern United States. *Agric. For. Meteorol.* **2017**, *247*, 414–423. [CrossRef]
91. Mo, K.C.; Lettenmaier, D.P. Heat wave flash droughts in decline. *Geophys. Res. Lett.* **2015**, *42*, 2823–2829. [CrossRef]
92. Hobbins, M.; Wood, A.; McEvoy, D.; Huntington, J.; Morton, C.; Verdin, J.; Anderson, M.; Hain, C. The Evaporative Demand Drought Index: Part I-Linking Drought Evolution to Variations in Evaporative Demand. *J. Hydrometeorol.* **2016**, *17*, 1745–1761. [CrossRef]
93. Stegehuis, A.I.; Vautard, R.; Ciais, P.; Teuling, A.J.; Jung, M.; Yiou, P. Summer temperatures in Europe and land heat fluxes in observation-based data and regional climate model simulations. *Clim. Dyn.* **2013**, *41*, 455–477. [CrossRef]
94. Teuling, A.J.; Seneviratne, S.I.; Stöckli, R.; Reichstein, M.; Moors, E.; Ciais, P.; Luyssaert, S.; van den Hurk, B.; Ammann, C.; Bernhofer, C.; et al. Contrasting response of European forest and grassland energy exchange to heatwaves. *Nat. Geosci.* **2010**, *3*, 722. [CrossRef]
95. Seneviratne, S.I.; Lehner, I.; Gurtz, J.; Teuling, A.J.; Lang, H.; Moser, U.; Grebner, D.; Menzel, L.; Schroff, K.; Vitvar, T.; et al. Swiss prealpine Rietholzbach research catchment and lysimeter: 32 year time series and 2003 drought event. *Water Resour. Res.* **2012**, *48*. [CrossRef]
96. Liu, Y.; Parolari, A.J.; Kumar, M.; Huang, C.-W.; Katul, G.G.; Porporato, A. Increasing atmospheric humidity and CO_2 concentration alleviate forest mortality risk. *Proc. Natl. Acad. Sci. USA* **2017**, *114*, 9918–9923. [CrossRef] [PubMed]
97. Ahmadi, B.; Moradkhani, H. Revisiting Hydrological Drought Propagation and Recovery Considering Water Quantity and Quality. *Hydrol. Proc.* **2019**, 1–14. [CrossRef]